Polymerization-Induced Viscoelastic Phase Separation in Polyethersulfone-Modified Epoxy Systems

Yingfeng Yu, Minghai Wang, Wenjun Gan, Qingsheng Tao, and Shanjun Li*

Department of Macromolecular Science and The Key Laboratory of Molecular Engineering of Polymer, Ministry of Education, Fudan University, Shanghai, 200433, China

Received: September 3, 2003; In Final Form: March 11, 2004

The polymerization-induced phase-separation process of polyethersulfone (PES)-modified epoxy systems was monitored in situ continuously on a single sample throughout the entire curing process by using optical microscopes, time-resolved light scattering (TRLS), scanning electronic microscopes (SEM), and a rheometry instrument. At specific PES content a viscoelastic transformation process of phase inversion morphology to bicontinuous was found with an optical microscope. The rheological behavior during phase separation corresponds well with the morphology development. Light-scattering results monitoring the phase-separation process of systems with final phase inversion morphology show a typical exponential decay procedure of scattering vector q_m. The characteristic relaxation time of phase separation can be described well by the WLF equation.

1. Introduction

Thermosets tend to have a characteristic low resistance to brittle fracture, and improving their fracture toughness by rubber modification is invariably accompanied by a significant drop in heat resistance. As a result, much work has been done to toughen highly cross-linked thermosetting polymers with high modulus, high glass transition temperature thermoplastics, such as polyethersulfone (PES),[1,2] polysulfone (PSF),[3] poly(ether ether ketone) (PEEK),[4] and polyetherimide (PEI).[5,6] With the increased amount of thermoplastics in modified thermoset systems, three kinds of morphologies have been observed, namely, thermoplastics particle, bicontinuous (or foamlike: sandwich for a co-continuous, double-phase structure consisting of a dispersion of macroscopic irregular domains showing a phase-inverted structure in a thermoset-rich matrix exhibiting a dispersion of thermoplastic-rich particles), and phase inversion (or spongelike: network-like for a dispersion of thermoset-rich matrix in a thermoplastic-rich matrix) structures.

Since the mechanical properties of the materials are determined by their final morphologies, much work has been focused on the mechanism study of phase separation and morphology control.[7−10] Effective improvement in toughness can only be obtained at high fractions of the engineering thermoplastic,[11−13] where the thermoplastic forms a continuous phase with the epoxy spherical domain, or the thermoplastic and epoxy form a bicontinuous phase structure. Thus it is essential to obtain a bicontinuous or phase-inversion morphology in material designing and property control.

Earlier works[14,15] suggested that the spinodal decomposition (SD) mechanism is most conceivable in thermoplastic modified thermoset systems due to the slow rate of nucleation growth (NG) during the curing process. However, studies of viscoelastic phase separation in polymer blends have changed this assumption recently. As these thermoplastic−solvent or thermoplastic−thermoplastic systems have been intensively investigated, and most of them are binary or ternary systems, such as PMMA(poly(methyl methacrylate)/PSAN(poly(styrene-*co*-acrylonitrile)),[16] PS(polystyrene)/PVME,[17] dextran/PEG(poly(ethylene glycol))/H_2O,[18] and polystyrene (PS)/poly(methylphenylsiloxane) (PMPS),[19] a series of viscoelastic phase separation theories are being developed to interpret the phenomena taking place in the thermoplastic−solvent or thermoplastic−thermoplastic systems.

Tanaka[20] found that if there is a large difference in the intrinsic dynamic asymmetry between the two components of blend, phase separation will be affected by the viscoelastic property, i.e., viscoelastic effects play a crucial role in the blends with "dynamic asymmetry". The dynamic asymmetry between constituent components in mixtures or solutions causes a coupling between stress and diffusion, which is due to an asymmetry stress division, thus inducing the abnormal phase structure like the spongelike phase inversion morphology. As a result, the phase separation process is determined by both the phase diagram and the ratio between fluctuation growth rate of the phase structure and the disentangle rate of the polymer chain for whatever phase separation mechanism, i.e., SD or NG.

For the blends of thermoplastic−thermosetting, phase separation is induced by the increasing molecular weight of thermosets. In this case, different phase morphologies can be obtained depending on the competition between the kinetics of phase separation and cross-linking chemical reaction, which are governed by the curing conditions, compositions, molecular weights, and molecular weight distributions of toughenners. Since there are large differences between thermoplastics and thermosets in both the molecular weights and glass transition temperatures, obviously, these blends should have dynamics asymmetry in the relaxation and diffusion of molecular chains.

Our previous works in poly(etherimide)-modified epoxy systems have found that the evolution of the light-scattering vector q_m during the late stage of spinodal decomposition follows the time−temperature superposition principle (WLF-like function).[21] The aim of our present work is to study whether the effect of viscoelasticity in thermoplastics-modified thermosets systems is a universal law or just by chance, and the chainwise polymerization-induced viscoelastic phase separation process

* Corresponding author. E-mail: sjli@fudan.edu.cn.

10.1021/jp036628o CCC: $27.50
Published on Web 04/22/2004

TABLE 1: The Composition of Modified Systems

blends	PES	DGEBA	MTHPA	BDMA
PES-14%	30	100	80	0.2
PES-20%	45	100	80	0.2

in the system of PES-modified epoxy cured with anhydride and tertiary amine was monitored by OM and SEM.

2. Experimental Section

Materials and Samples Preparation. The epoxy oligomer DER 331 was provided by Dow Chemical Co. and is a low molecular weight liquid diglycidyl ether of bisphenol A (DGEBA) with an epoxide equivalent of 182−192. Hydroxyl-terminated polyethersulfone (PES) were supplied by Jilin University, China, which has a weight-average molecular weight of 3.4×10^4 g/mol and polydispersity of 3.6 (T_g = 188 °C). The curing agent is methyl tetrahydrophthalic anhydride (MTHPA), HY 918, Ciba-Geigy. The initiator is benzyldimethylamine (BDMA) from Shanghai Third Reagent Factory.

The homogeneous mixture of PES/DGEBA was prepared by adding PES to the stirring epoxy monomer at 150 °C under nitrogen gas, after the mixture had cooled to 80 °C, MTHPA and BDMA were added and the mixture was stirred vigorously for 2 min until MTHPA and BDMA were completely dissolved. The samples were degassed under vacuum for another few minutes afterward and then cast immediately onto glass slides. Two blends were studied in this work as listed in Table 1. In PES-14% systems, PES has a weight percent of 14.3%, while in PES-20%, PES has a weight percent of 20%.

Measurements. A Setaram Differential Scanning Calorimetry (DSC92) instrument was used for cure reaction and T_g detection. Philip XL 39 scanning electronic microscopes (SEM) were employed to examine morphologies of the fracture surfaces of cured specimens. The melt viscosity variations of the blends during cure reaction were recorded on an Ares-9A rheometry instrument: about 1 g of the blend was sandwiched between two round fixtures and softened at 60 °C for 2 min. The plate distance was then adjusted to about 1.5 mm and the temperature was raised quickly at a rate of 100 deg/min to the preset curing temperature. All the blends were tested under a parallel plate mode with a controlled strain of 1% and test frequency of 1 Hz to ensure that measurements were performed under dynamic equilibrium conditions. The phase-separation process during the isothermal curing reaction was observed at real time and in situ on the self-made time-resolved light scattering (TRLS) instrument with controllable hot chamber and with the TRLS technique described elsewhere.[21] The change of the light-scattering profiles was recorded at appropriate time intervals during isothermal curing. The blend of epoxy monomer with PEI for TRLS observation was prepared by melt-pressing the film. A sample was observed in situ with an Olympus Invented Microscope PMG3 while being cured in a hot chamber at 120 °C.

3. Results and Discussion

Development of Phase Structure. SEM morphologies of fractured surfaces of the two final cured compositions are shown in Figure 1. The blend PES-20% displays a phase inversion structure as shown in Figure 1a, in which spherical epoxy-rich particles of regular diameter about 1−3 mm disperse in the membrane-like PES-rich matrix. The blend PES-14% (Figure 1b) shows bicontinuous morphologies of different sizes, in which the epoxy-rich particles of diameter also about 2−4 mm disperse in the PES-rich continuous region while a few irregular PES-rich particles disperse in the epoxy-rich region.

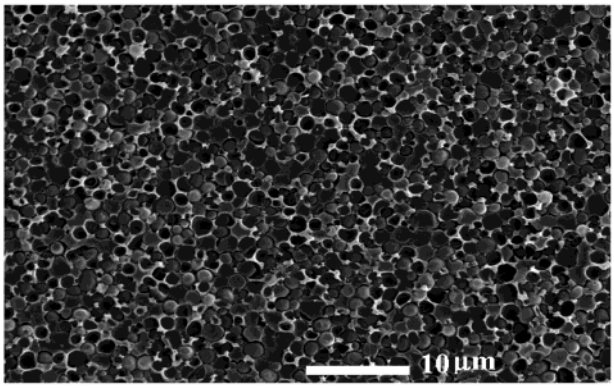

(a)

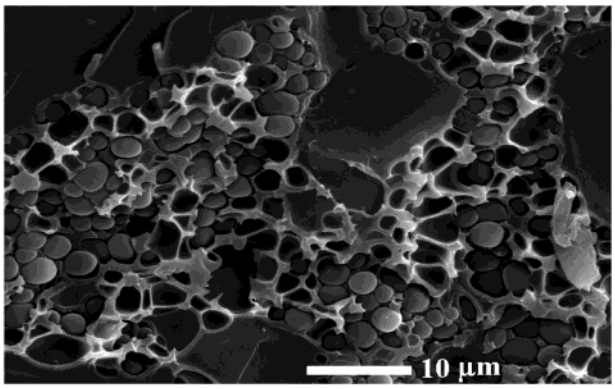

(b)

Figure 1. SEM of two blends cured at 120 °C for 5 h: (a) PES-20% and (b) PES-14%.

A clear transformation process for the initial phase inversion morphology after the cloud point to the final bicontinuous phase structure was found with an optical microscope as shown in Figure 2, in which the evolution of the bicontinuous structure in the PES-14% blend cured at 120 °C was observed in situ continuously.

The cloud-point time was about 9 min and the first micrograph with enough contrast between phases was recorded 1 min after the beginning of phase separation (Figure 2a). The epoxy droplets formed first have an average size in the order of 10^2 mm. The fractured surface of another sample at the same conditions was also observed by SEM as shown in Figure 3a. A phase-inversion structure was observed by both optical micrograph and SEM in which the epoxy spheres are surrounded by the membrane-like PES-rich phase and some large epoxy droplets of diameter about 8−15 mm also exist. As the polymerization proceeds, larger epoxy droplets appear, grow ever larger, connect to each other, and become the continuous phase structure then form the bicontinuous phase structure at last.

Although the development of the bicontinuous structure in the polymerization-induced phase separation process was reported earlier[22] in polysulfone-modified epoxy systems, and double phase separation happened in some systems also due to viscoelastic effects.[20] After the investigations by both the OM and SEM in our systems, it was found that they are viscoelactic phase-separation processes as reported previously in the thermally induced phase-separation process of polymer−solvent or polymer−polymer systems.

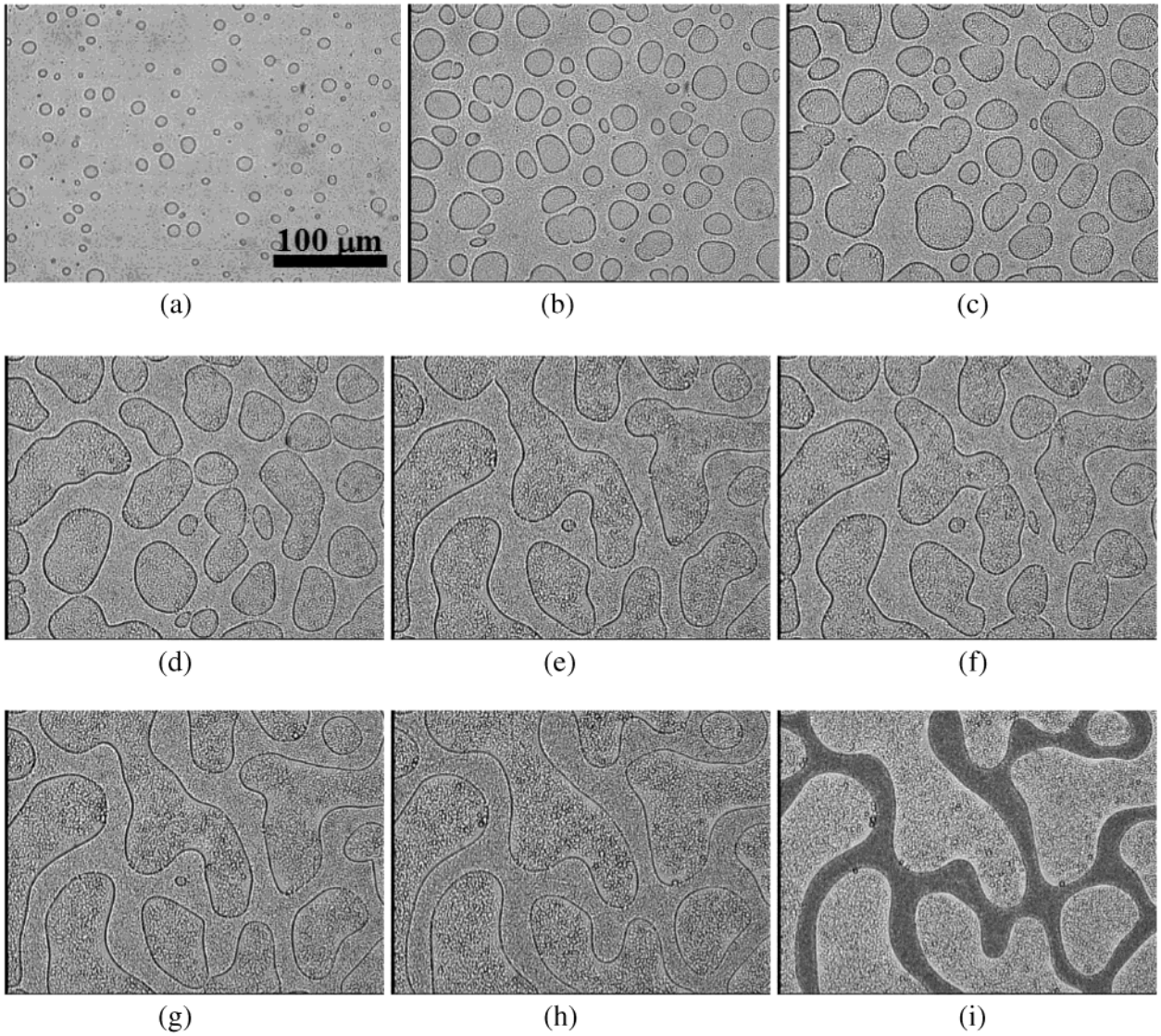

Figure 2. Development of morphologies in a PES-14% blend cured at 120 °C, followed by optical microscopy: (a) 600 s, (b) 660 s, (c) 720 s, (d) 780 s, (e) 840 s, (f) 900 s, (g) 960 s, (h) 1200 s, and (i) 3600 s.

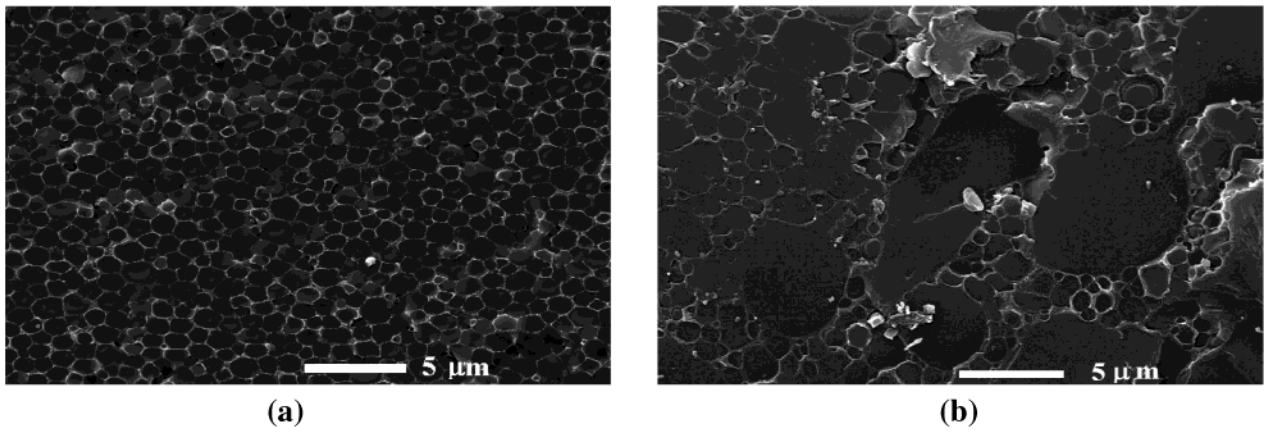

Figure 3. SEM of PES-14% cured at 120 °C for different times: (a) 480 s and (b) 600 s.

Both OM and SEM results following PES-14% and PES-20% systems verify that the initial morphology is phase inversion as shown in Figures 2 and 3. In PES-20% systems, with polymerization proceeding epoxy particles grow larger and the volume fraction of PES decreases due to phase separation as the membrane-like PES region becoming thinner and thinner. For the PES-14% system, PES concentration is not high enough to keep its inversed structure, and as a result epoxy domains coalesce and generate into the continuous structure and form the bicontinuous morphology.

A regular lattice of fine particles or the second phase-like domains in all phases is observed in all optical micrographs. To investigate this phenomenon, samples cured for 480 and 600 s at the same conditions were studied by SEM. As shown in

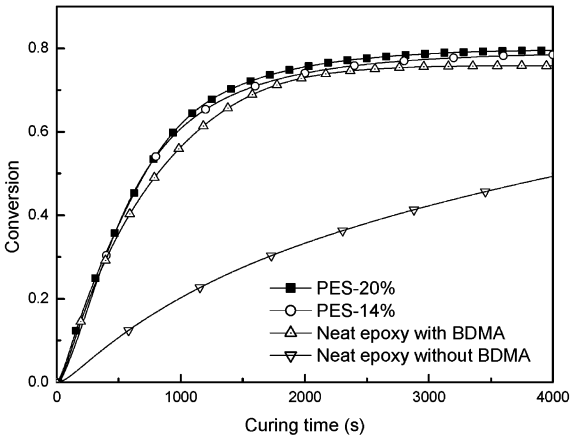

Figure 4. Isothermal cure behavior of PES-modified systems and neat epoxy systems with and without initiator BDMA cured at 150 °C.

Figure 3, there are few irregular PES particles in the epoxy large particles and the continuous region during the growth of epoxy particles. Thus the regular lattice is only an illusion of the optical micrograph.

Cure and Rheological Behavior. Isothermal DSC curves of the two blends, neat epoxy with and without initiator BDMA cured at 150 °C, are shown in Figure 4. The introduction of initiator tertiary amine increased sharply the cure rate and final conversion. Pure epoxy−anhydride systems react very slowly and reaction occurs due to partial hydrolysis of anhydride leading to an epoxy-acid stepwise reaction, while tertiary amine coupled with anhydride/hydroxyl groups initiates the chainwise reaction.[23−25] However, the addition of PES has few effects on the cure rate and conversion; the cure rates of PES-14% and PES-20% are slightly higher than that of neat epoxy with BDMA. The role of the hydroxyl-terminated PES, according to several workers,[23−25] is to co-initiate the chainwise reaction due to the existence of the hydroxyl group and to retard polymerization due to the effect of dilution.[9,24]

To better understanding the effects of initiator tertiary amine on the cure mechanism, DSC curves of PES-14% and the sample without initiator BDMA at variations of heating rate were studied as shown in Figure 5. According to the Kissinger equation[26]

$$\frac{\mathrm{d}(\ln\beta/T_\mathrm{p}^{\,2})}{\mathrm{d}(1/T_\mathrm{p})} = -\frac{E_\mathrm{a}}{R} \qquad (1)$$

where β is the heating rate, T_p the maximum temperature of the exothermic peak, E_a the apparent activation energy, and R the gas constant. The apparent activation energies of the cure reaction for PES-14% and sample without initiator BDMA are 92.3 and 67.4 kJ/mol, which accords with literature[23,24] due to different polymerization mechanisms, in other words, the former is a chainwise polymerization, where the tertiary amine is an initiator, and the latter is a stepwise polymerization.

In Figure 6 the complex viscosity η^* of the two blends and neat epoxy were plotted at the same curing temperature. As one can see, at the beginning of the cure reaction, the blends behaved as semidilute polymer solutions having viscosities lower than 5 Pa·s (PES-20% < 3 Pa·s, PES-14% < 2 Pa·s) at the curing temperature of 120 °C and the enlargement of PES concentration enhanced the initial viscosity.

When phase separation occurred, η^* increased quickly in both of the blends while the viscosity of neat epoxy remained almost unchanged at the same time (conversion) scale. For the PES-20% system, the viscosity increased gradually after the initial phase separation. However, more complex behaviors were observed in the PES-14% system, which had final bicontinuous phase structures as shown in Figure 1: after the viscosity jumping at the cloud point, a decrease of viscosity was found and after that the viscosity increased again.

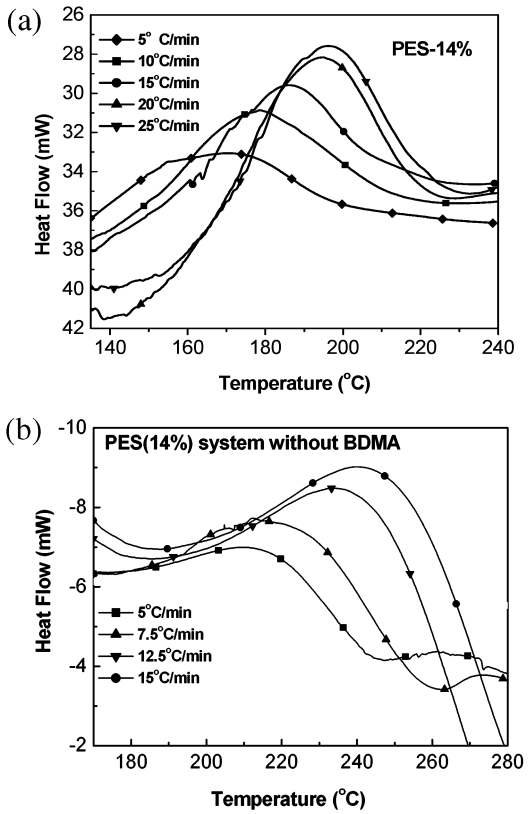

Figure 5. DSC curves of PES (14%)-modified systems with and without initiator BDMA at different heating rates.

To get a clear relationship between rheological behavior and the phase structure, T_g values of samples cured for different times were measured by DSC. It was found that phase separation took place with both viscosity and G' increase, while two T_g values corresponding to two phases are detected later at about 600 s (conversion = 0.09) due to the measurement limiting of DSC in Figure 6b. Compared with the neat epoxy system cured at the same temperature, there is little change in viscosity (lower than 1 Pa·s) at the same conversion, in other words, the viscosity increase after phase separation was caused by the formation of the PES-rich matrix, and the decrease of viscosity in PES-14% was caused by the formation of the biscontinues structure. At first, T_g of the PES-rich matrix increased quickly during phase separation while T_g of the epoxy-rich matrix changed slightly, and after the vitrification of the PES-rich matrix (T_g reached the cure temperature, Berghmans' point, at about 1200 s, conversion = 0.19), T_g of the epoxy-rich matrix increased at about 1500 s (conversion at about 0.23) due to gelation of the epoxy system as compared to the rheological study of neat epoxy.

Ishii et al.[27] have studied the gelation mechanism in PPE/epoxy blend and found that the gelation of PPE/epoxy blends is the vitrification of a PPE-rich matrix following phase separation and not chemical gelation of neat epoxy (epoxy-rich). In our work, the cross point of G' and G'' (gel point, congruency of tanδ with frequency) in PES-20% (and PES-14%) might be caused by the vitrification of the PES-rich phase since the T_g values of the PES-rich matrix reached the cure temperature at about this time. But that gelation of the epoxy-rich matrix

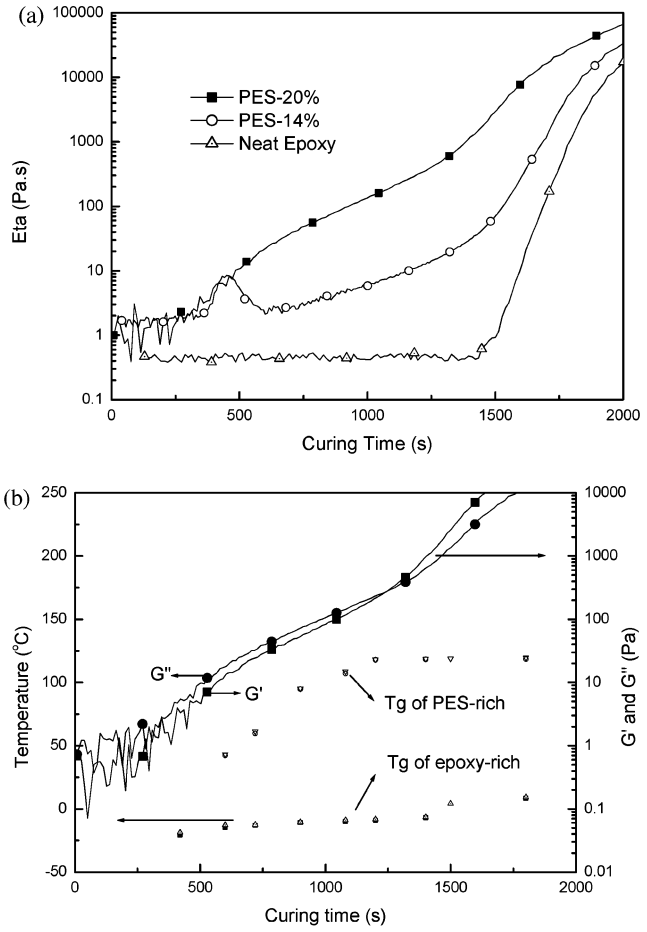

Figure 6. Influence of PES concentration on the rheological behavior. (a) Variation of complex viscosity η^* in PES-14%, PES-20%, and neat epoxy systems cured at 120 °C; (b) G' and G'' of PES-20% and T_g evolution of PES-20% and PES-14%.

happened before vitrification of the thermoplastic-rich matrix was reported in the literature.[28] The vitrification of the PES-rich matrix was slightly earlier than the chemical gelation of the epoxy-rich matrix (T_g of the epoxy-rich matrix increased quickly[28]) according to the rheological study of neat epoxy resin and DSC studies of the blends. And the second quick increase of viscosity in PES-20% and PES-14% was caused by the chemical gelation of the epoxy-rich matrix[28,29]as it was in the same time (conversion) scale of the neat epoxy system.

Time−Temperature Equivalency of TRLS Results. The phase-separation process of all modified systems was monitored in situ by TRLS. The change of the light-scattering profiles was recorded at appropriate time intervals during isothermal curing at temperatures from 80 to 150 °C with an interval of 10 °C. At all the temperatures, PES-14% systems show little change of light-scattering profiles (only changes in light intensity, and the reason will be discussed in the Viscoelastic Phase Separation section), while for PES-20% systems, various peak scattering vector q_m values corresponding to an instantaneous I_m varied with time are obtained from the light-scattering profiles. As an example, Figure 7 shows profiles for the PES-20% system cured at 130 °C isothermally.

After the beginning of phase separation, the scattering vector with maximum scattering intensity, q_m, appeared and then decreased with time, while the relative intensity of scattered light increased continually from the beginning of the phase separation. It was observed that they exhibit similar characteristics at all the temperatures cured.

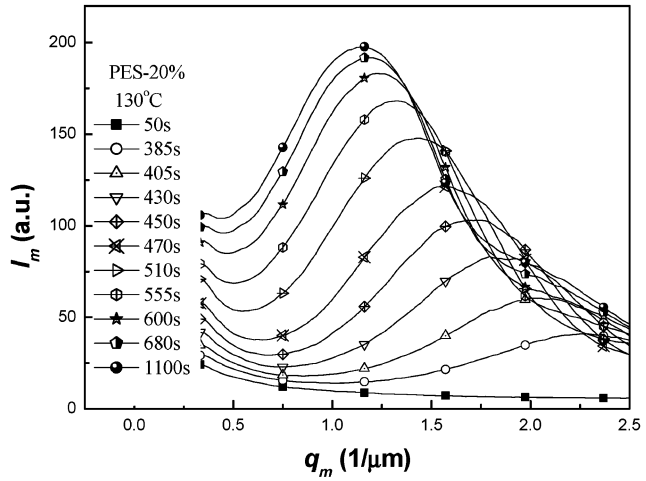

Figure 7. TRLS profiles for the PES-20% system cured at 130 °C isothermally.

As curing temperature increases, both the CP time and the elapsed time between the onset of phase separation and morphology fixation are shortened due to the higher rate of the epoxy−anhydride reaction at higher temperatures, i.e., the phase separation takes place early and winds up more quickly as shown in Table 2. It was founded that x-CP gets slightly higher at both low (80, 90 °C) and high temperature (140, 150 °C), and the reason might be that the LCST behavior caused higher conversion at the low temperature[14,15] while the deep quench due to cure rate much faster than diffusion rate induced later phase separation at the higher temperature.

As shown in Figure 8, a typical exponential decay of scattering vector q_m is found by calculation of TRLS results of the PES-20% system at 120 °C according to eq 2 as an example.

$$q_m(t) = q_0 + A_0 \exp(-t/\tau) \tag{2}$$

As $t = \infty$, $q_m = q_0$. Here A_0 is the magnifier, and τ is the relaxation time of phase separation and could indicate the coarsening capability of epoxy droplets. The values at different temperatures are reported in Table 2.

Since the correlation coefficient R^2 varied between 0.974 and 0.998, the results can be thought as believable. The parameter τ obtained in Table 2 is obtained by simulation of the epoxy droplets coarsening process. It is obvious that the relaxation time τ decreases with the increase of curing temperature. Compared with the results of the T_g changes of two phases during the phase-separation process, it was found that the evolution of q_m corresponds to the change of PES-rich T_g during phase separation, and the vitrification of the PES-rich phase (PES-rich T_g equals the cure temperature), which stops diffusion, corresponds to the end of q_m change. The relaxation behavior of q_m was caused by lowering the diffusion rate of epoxy monomers (viscoelastic flow) from those of the PES-rich phase with a gradual increase in concentration, which transferred the PES-rich phase from viscous flow to elastic and finally to the glass state. Whether or not the relaxation behavior of q_m would happen in the systems with earlier gelation of thermoset than vitrification of the thermoplastic-rich phase needs further study.

Because the relaxation time τ indicates the coarsening capability of epoxy droplets, it may correspond to the characteristic relaxation time of PES, epoxy monomer, or growing epoxy in the pseudoternary blend; but the chain motilities of PES, epoxy monomer, and growing epoxy are very different. As most of the epoxy monomer remains unchanged (x-CP at

TABLE 2: Results Obtained by TRLS for PES-20%

temp (°C)	τ (s)	R^2 [a]	t-CP (s)[b]	x-CP[b]	t-End[c]	x-End[c]
150	39.6 ± 0.8	0.998	280 ± 10	0.21 ± 0.005	460 ± 20	0.35 ± 0.01
140	60 ± 1	0.998	320 ± 10	0.12 ± 0.002	660 ± 20	0.28 ± 0.01
130	102 ± 2	0.998	390 ± 10	0.09 ± 0.002	810 ± 20	0.21 ± 0.01
120	135 ± 3	0.996	750 ± 20	0.10 ± 0.002	1250 ± 40	0.19 ± 0.01
110	208 ± 4	0.998	920 ± 20	0.09 ± 0.002	2930 ± 50	0.21 ± 0.01
100	611 ± 12	0.993	2550 ± 50	0.11 ± 0.005	4320 ± 50	0.20 ± 0.01
90	1330 ± 25	0.985	7280 ± 100	0.12 ± 0.005	11160 ± 100	0.19 ± 0.01
80	3240 ± 65	0.974	10450 ± 200	0.13 ± 0.005	28740 ± 200	0.19 ± 0.01

[a] Correlation coefficient. [b] t-CP, x-CP: the time and curing conversion of initial phase separation observed by TRLS. [c] t-End, x-End: the time and curing conversion when q_m remains constant observed by TRLS.

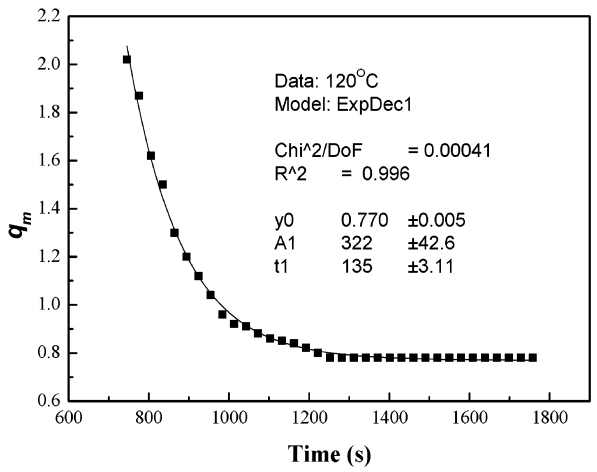

Figure 8. TRLS profiles of the PES-20% system, q_m, versus time at 120 °C. The points correspond to the experiment data and the line corresponds to the result simulated by $q_m(t) = q_0 + A_0 \exp(-t/\tau)$.

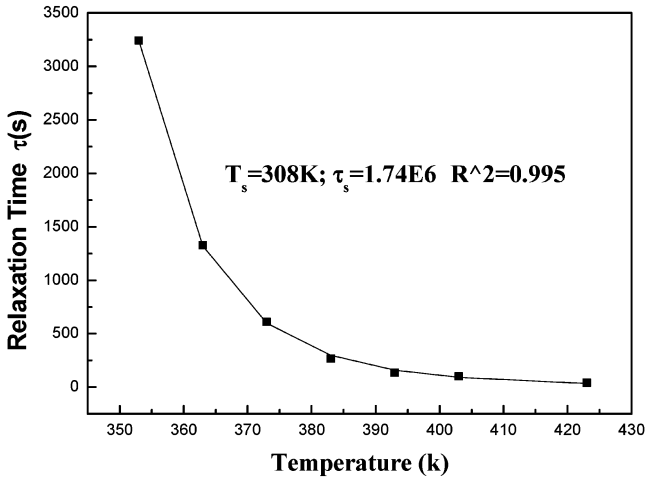

Figure 9. Plots of the relaxation time τ versus temperature. The points correspond to experimental data and the line corresponds to results simulated by $\tau = \tau_s \exp[-\ln 10 \times 8.86 \times (T - T_s)/(101.6 + (T - T_s))]$.

about 0.1 and x-END at about 0.2) during the phase-separation process, then the relaxation time τ may be regarded as the viscous flow capability of epoxy monomer or growing-thermoset (low molecular weight) droplets. It is understandable when the blend cure at a higher temperature, the diffusion rate of the thermoset monomer, or the growing thermoset increase and impel the PES and growing epoxy chain to disentangle then two or more epoxy droplets combine more quickly.

The Williams−Landel−Ferry (WLF) Function. For the further verification of the viscoelastic behavior of this system, the relaxation time τ versus temperature T listed in Table 2 was simulated by the Williams−Landel−Ferry (WLF) equation $\log(\tau/\tau_s) = (-C_1(T - T_s)/C_2 + (T - T_s))$. Assuming that $C_1 = 8.86$ K and $C_2 = 101.6$ K, the WLF equation can be written as

$$\tau = \tau_s \exp[-\ln 10 \times 8.86 \times (T - T_s)/(101.6 + (T - T_s))] \quad (3)$$

As showed in Figure 9, the simulation results give a good fit to the experimental data. This means that the relaxation time obeys the time−temperature superposition (TTS) principle and can be described by the Williams−Landel−Ferry (WLF) function. The values T_s and τ_s obtained from simulation are 307.8 K and 1.74×10^6 for the PES-20% system.

For verification, we calculate the shifting factor α_T ($= \tau/\tau_s$) at varied temperature and T_s. Figure 10 shows the plots of $1/\log(\alpha_T) - 1/(T - T_s)$ of the blend. It is obvious that the linear function undoubtedly exists. In addition, similar nonlinear thermally induced phase-separation behavior in PMMA/SAN binary polymer blends was also described by the WLF-like function in Zheng's work.[30]

According to the WLF equation, when C_1 and C_2 are selected as the empirical constants 8.86 and 101.6 K, the T_s may be

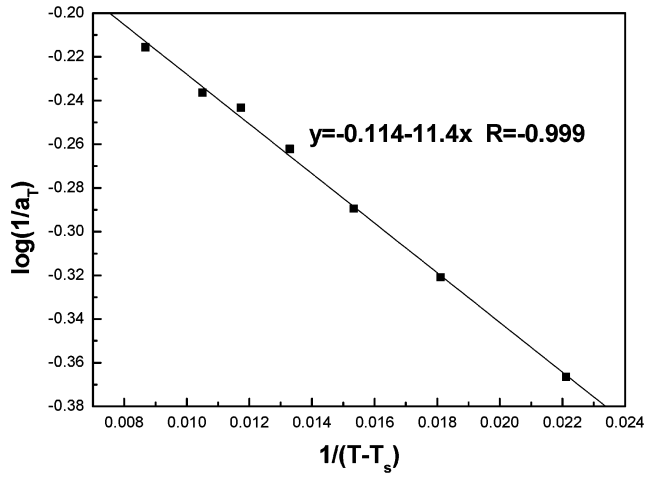

Figure 10. The plots of $1/\log(\alpha_T)$ versus $1/(T - T_s)$ for PES-20%.

related to the flow temperature of the polymer chain, which should be 50 °C higher than T_g of this polymer. Thus, to discuss the meaning of T_s, T_g values of the epoxy−anhydride without PES were measured by DSC at different heating rates (in Figure 11). It is reasonable to eliminate the effect of heating rate on T_g by extrapolating the heating rate to zero. Thus T_g of the blend is 248.2 K. This implies that the coarsening process at the late stage SD is mainly controlled by the viscoelastic flow of epoxy monomers.

Viscoelastic Phase Separation. It is common knowledge that thermoplastic concentration has a strong influence on both the final morphology and the phase-separation mechanism of the modified system. Systems with thermoplastic continuous structures, i.e., bicontinuous and phase-inversion structures, were

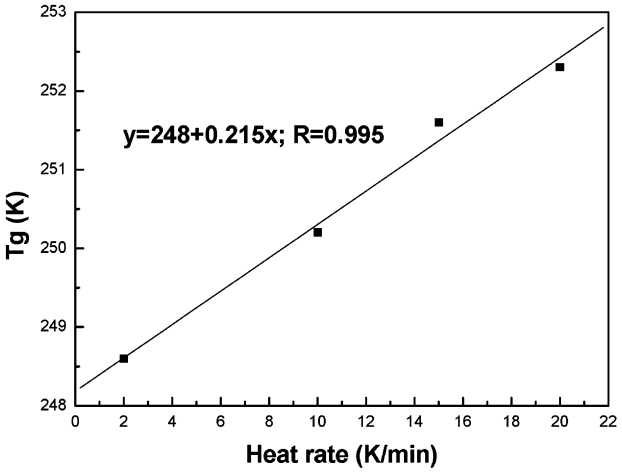

Figure 11. T_g values of epoxy-anhydride without PES were measured by DSC at different heating rates.

chosen to study their phase-separation mechanisms due to their good mechanical properties.

For the chainwise polymerization reaction, the systems are quite complicated as the pseudoternary blend: PES/growing-thermoset/and monomers. At low conversion (before gelation), the molecular weight of the growing-thermoset distributed with Poisson distribution[31,32] and increased with conversion[32] by GPC studies. As a result, the growing-thermoset could be simplified as a polymeric component with an average polymerization degree of n_{gt} and volume fraction of ϕ_{gt} in terms of the Flory−Huggins theory,[33] and the mixing free energy F of the blend can be given by:

$$\frac{F}{kT} = \sum_{1}^{r} \frac{\phi_i}{n_i} \ln \phi_i + \sum_{i<j}^{r}\sum^{r} \chi_{ij} \cdot \phi_i \cdot \phi_j \qquad (4)$$

where n_i is the weight average polymerization degree of component i, ϕ_i the volume fraction, and χ_{ij} the Flory−Huggins interaction parameter. Since the statistical approach to the average molecular weight and distributions of molecular sizes of the thermoset monomer (including hardeners) are kept unchanged during chainwise polymerization at low conversion before gelation, thermoset monomers can be simplified as a component or a solvent ($n_s = 1$) at the early stage of phase separation. Although the effects of polydispersion of all three components were neglected, it does not mean at all that they are insignificant.[34] As did Tompa,[35] we assumed that there is no interaction between the thermoset monomer and growing-thermoset and the interaction between a segment of thermoplastic (n_p, ϕ_p) and a solvent molecule is the same as that between segments of the two polymers.

The spinodial is given by

$$(1 - 2\chi n_p \phi_p)[1 - 2\chi(\phi_s + n_{gt}\phi_{gt})] = 1 \qquad (5)$$

And the critical point is determined from

$$n_{gt}(1 - \phi_p)(1 - 2\chi n_p \phi_p)^3 + (n_{gt} + 1)n_p \phi_p (1 - 2\chi n_p \phi_p)^2 - n_p{}^2 \phi_p = 0 \qquad (6)$$

The critical values of χ_c, which marked the threshold at which immiscibility sets in, are obtained with the following:

$$\chi_c = {}^1/_2(n_{pt}{}^{-1/2} + n_p{}^{-1/2})^2 \qquad (7)$$

Provided that χ is not influenced by the curing reaction at the same curing temperature, immiscibility is caused by the entropy reduction due to the molecular weight increase of the growing-thermoset, n_{gt}, thus χ_c equals χ_0. For a specific MW of thermoplastic, n_p, we obtain the following equation

$$n_{gtc} = n_p/[(2n_p\chi_0)^{1/2} - 1]^2 \qquad (8)$$

That is, with an increase of n_p, the critical value of n_{gtc} drops rapidly, while the Flory−Huggins interaction parameter χ, which is a function of temperature, increases with cure temperature in a LCST system and thus causes earlier x-CP when kinetic factors are minimized.

When compared to the TRLS changes in PES-20% systems there is no sign of light-scattering profiles, but light intensity slowly growing was observed by TRLS in PES-14% systems, i.e., the phase separation mechanism of PES-20% is SD while that of PES-14% is NG, since SD causes a regular phase structure and can be detected by TRLS. That is, whatever the phase-separation mechanism, i.e., SD or NG, in viscoelastic phase separation the initial morphology during phase separation is the phase-inversion structure due to the large difference between thermoplastics and slightly cured thermoset phases in both molecular weight and chain mobility.

From the theoretical point of view of both thermodynamic and dynamic analysis, lowering PES dosage favors the formation of the epoxy matrix. Moreover, based on the theories of viscoelastic phase separation,[20] lowering PES concentration will decrease dynamic asymmetry between thermoplastics and the growing thermoset/thermoset monomer and thus facilitate the thermoset of shorter relaxation time forming continuous morphology. The characteristic rheological times for the epoxy-rich and thermoplastic-rich phases, τ_t^{sr} and τ_t^{pr}, are[36]

$$\tau_t^{sr} \approx n_p{}^2 b^2/(3\pi kT) \qquad (9)$$

$$\tau_t^{pr} \approx \eta b^3 n_p{}^3 (\phi_{pr})^{\alpha}/(kT) \qquad (10)$$

where η is the viscosity and b is the length of a unit monomer. If $\tau_t^{pr}/\tau_t^{sr} \approx n_p \cdot \phi_{pr}{}^2$ is defined as the dynamic asymmetry parameter for an unstable state (phase separation), we find that the increase of PES volume fraction ϕ_{pr} will enhance dynamic asymmetry and favor the formation of the PES matrix.[20] On the basis of the model of Tanaka,[20] the domain deformation process can be characterized by two time scales τ_d (characteristic time of deformation) and τ_{ts} (characteristic rheological time of the slower phase). τ_d decreases rapidly with the composition difference at first and then increases with the domain size, while τ_{ts} increases steeply with the composition difference and becomes almost constant in the late stage. Viscoelastic phase separation can thus be classified into three regimes: initial stage ($\tau_d > \tau_{ts}$), elastic regime ($\tau_d < \tau_{ts}$), or hydrodynamic regime ($\tau_d > \tau_{ts}$).

In the present dynamic asymmetry systems of PES and thermoset monomer/growing thermoset, in the middle and late stage of phase separation, the slower dynamic phase (PES-rich phase) becomes more and more viscoelastic with the escape of thermoset monomer (or low MW growing thermoset) from the PES-rich phase and eventually behaves as an elastic body. Meanwhile, the less viscoelastic phase (thermoset-rich phase) starts to coarsen with time and the elastic force balance dominates the morphology instead of the interface tension, which leads to the anisotropic shape of the domain. This is in accord with the elastic regime ($\tau_d < \tau_{ts}$). As the rate of curing reaction is slow enough, the coarsening process proceeds further and

phase separation drops into the hydrodynamic regime ($\tau_d > \tau_{ts}$) where disentanglement of PES chains occurs in PES-14%. The anisotropic shape of the domain becomes spherical again with the lowest interfacial energy since the interface energy overcomes the elastic energy. While the coarsening of thermoset-rich particles made the thermoset-rich phase become a continuous structure, further phase separation or disentanglement of PES chains slowed down in the region of the PES-rich phase.

4. Conclusion

A viscoelastic phase-separation process for the initial phase inversion morphology near the cloud point to the final bicontinuous phase structure was found with an optical microscope in thermoplastic modified thermoset systems. The rheological behavior evolution corresponds well with the morphology variation. TRLS results from monitoring the phase-separation process of systems with phase inversion morphologies show a typical exponential decay procedure of both light intensity I_m and vector q_m. The characteristic relaxation time of phase separation can be described well by the WLF equation, and DSC results demonstrated that the characteristic relaxation time of phase separation corresponds to that of the chain segments of thermoset.

Acknowledgment. This research work was supported by the National Nature Science Foundation of China (Grant 50273007).

References and Notes

(1) Bucknall, C. B.; Gomez, C. M.; Quintard, I. *Polymer* **1994**, *35*, 353.
(2) Chen, Y. S.; Lee, J. S.; Yu, T. L.; Chen, J. C.; Chen, W. Y.; Cheng, M. C. *Macromol. Chem. Phys.* **1995**, *196*, 3447.
(3) Min, B. G.; Hodgkin, J. H.; Stachurski, Z. H. *J. Appl. Polym. Sci.* **1993**, *50*, 1065.
(4) Bennett, G. S.; Farris, R. J.; Thompson, S. A. *Polymer* **1991**, *32*, 1633.
(5) Riccardi, C. C.; Borrajo, J.; Williams, R. J. J.; GirardReydet, E.; Sautereau, H.; Pascault, J. P. *J. Polym. Sci. Polym. Phys.* **1996**, *34*, 349.
(6) Bonnet, A.; Pascault, J. P.; Sautereau, H.; Taha, M.; Camberlin, Y. *Macromolecules* **1999**, *32*, 8517.
(7) Yu, Y. F.; Cui, J.; Chen, W. J.; Li, S. J. *J. Macromol. Sci. Chem.* **1998**, *A35*, 121. Cui, J.; Yu, Y. F.; Li, S. J. *J. Macromol. Sci. Chem.* **1998**, *A35*, 649.
(8) Cui, J.; Yu, Y. F.; Chen, W. J.; Li, S. J. *Macromol. Chem. Phys.* **1997**, *198*, 3267. Cui, J.; Yu, Y. F.; Li, S. J. *Macromol. Chem. Phys.* **1998**, *199*, 1645.
(9) Zhang, Z. C.; Cui, J.; Li, S. J.; Sun, K.; Fan, W. Z. *Macromol. Chem. Phys.* **2001**, *202*, 126. Yu, Y. F.; Zhang, Z. C.; Gan, W. J.; Li, S. J. *Ind. Eng. Chem. Res.* **2003**, *42*, 3250.
(10) Wu, X. G.; Cui, J.; Ding, Y. F.; Li, S. J.; Dong, B. Z.; Wang, J. *Macromol. Rapid Commun.* **2001**, *22*, 409.
(11) Girard-Reydet, E.; Vicard, V.; Pascault, J. P.; Sautereau, H. *J. Appl. Polym. Sci.* **1997**, *65*, 2433.
(12) Kim, S. C.; Brown, H. R. *J. Mater. Sci.* **1987**, *22*, 1589.
(13) Cho, J. B.; Hwang, J. W.; Cho, K.; An, J. H.; Park, C. E. *Polymer* **1993**, *34*, 4832.
(14) Yamanaka, K.; Inoue, T. *Polymer* **1989**, *30*, 662.
(15) Inoue, T. *Prog. Polym. Sci.* **1995**, *20*, 119.
(16) Pathak, J. A.; Colby, R. H.; Kamath, S. Y.; Kumar, S. K.; Stadler, R. *Macromolecules* **1998**, *31*, 8988.
(17) Polios, I. S.; Soliman, M.; Lee, C.; Gido, S. P.; Rohr, K. S.; Winter, H. H. *Macromolecules* **1997**, *30*, 4470.
(18) Hopkinson, I.; Myatt, M. *Macromolecules* **2002**, *35*, 5153.
(19) Karatasos, K.; Vlachos, G.; Vlassopoulos, D.; Fytas, G.; Meier, G.; Du Chesne, A. *J. Chem. Phys.* **1998**, *108*, 5997.
(20) Araki, T.; Tanaka, H. *Macromolecules* **2001**, *34*, 1953. Tanaka, H.; Miura, T. *Phys. Rev. lett.* **1993**, *71*, 2244. Tanaka, H.; Araki, T. *Phys. Rev. lett.* **1997**, *78*, 4966. Tanaka, H. *J. Phys.*: *Condens. Matter* **2000**, *12*, R207. Tanaka, H.; Araki, T. *Phys. Rev. Lett.* **1998**, *81*, 389.
(21) Gan, W. J.; Yu, Y. F.; Wang, M. H.; Tao, Q. S.; Li, S. J. *Macromolecules* **2003**, *36*, 7746.
(22) Oyanguren, P. A.; Galante, M. J.; Andromaque K.; Frontini, P. M.; Williams, R. J. J. *Polymer* **1999**, *40*, 5249.
(23) Antoon, M. K.; Koenig, J. L. *J. Polym. Sci.*: *Polym. Chem.* **1981**, *19*, 549.
(24) Woo, E. M.; Seferis, J. C. *J. Appl. Polym. Sci.* **1990**, *40*, 1237.
(25) Montserrat, S.; Flaqué, C.; Calafell, M.; Andreu, G.; Málek, J. *Thermochim. Acta* **1995**, *269*−*270*, 213.
(26) Kissinger, H. E. *Anal. Chem.* **1957**, *29*, 1702.
(27) Ishii, Y.; Ryan, A. J. *Macromolecules* **2000**, *33*, 167.
(28) Bonnet, A.; Pascault, J. P.; Sautereau, H. *Macromolecules* **1999**, *32*, 8524. Paul, D. R.; Bucknall, C. C. *Polymer blends*; Formulation, Vol. 1; John Weiley&Sons: New York, 2000.
(29) Kim, H. K.; Char, K. K. *Ind. Eng. Chem. Res.* **2000**, *39*, 955.
(30) Zheng, Q.; Peng, M.; Song Y. H.; Zhao, T. J. *Macromolecules* **2001**, *34*, 8483.
(31) Nielsen, J. A.; Chen, S. J.; Timm, D. C. *Macromolecules* **1993**, *26*, 1369.
(32) Wei, C. Ph.D. Dissertation, The University of Nebraska−Lincoln, 2002, ProQuest Information and Learning.
(33) Flory, P. J. Principles of Polymer Chemistry, Cornell University Press: New York, 1953.
(34) Tanaka, M.; Hashimoto, T. *Phys. Rev. E* **1993**, *48*, 647.
(35) Tompa, H. *Trans. Faraday Soc.* **1949**, *45*, 1142.
(36) Tanaka, H. *J. Chem. Phys.* **1995**, *103*, 2361.